ELSEVIER

Fluid Phase Equilibria 167 (2000) 145–159

FLUID PHASE EQUILIBRIA

www.elsevier.nl/locate/fluid

Prediction of solid–fluid phase diagrams of light gases–heavy paraffin systems up to 200 MPa using an equation of state–G^E model

Jérôme Pauly [a], Jean-Luc Daridon [a,*], Joao A.P. Coutinho [b], Niels Lindeloff [c], Simon I. Andersen [c]

[a] *Laboratoire des Fluides Complexes, Groupe Haute Pression, Université de Pau, BP 1155, 64013 Pau Cedex, France*
[b] *Centro de Investigação em Química, FCUP, Departamento de Quimica da Universidade de Aveiro, 3810 Aveiro, Portugal*
[c] *Department of Chemical Engineering, Technical University of Denmark, DK-2800 Lyngby, Denmark*

Received 11 September 1999; accepted 21 October 1999

Abstract

This paper presents a procedure for the simultaneous prediction of fluid–fluid and solid–fluid equilibria of light gases–heavy hydrocarbons systems under pressure. The fluid phases behaviour is described by the modified LCVM, an equation of state–G^E model and the solid phase non-ideality is represented by the Wilson equation using the predictive local composition concept.

This procedure was tested for several binary and ternary systems as well as multi-component systems leading to a good representation of both fluid–fluid and solid–fluid equilibria with a typical average absolute deviation of 1.5 K for the solid–fluid phase boundary of binary and ternary mixtures and of 0.5 K for multi-component systems. The AAD% in the fluid–fluid phase boundary of multi-component systems is of 3.2%.

Keywords: Solid–liquid equilibrium; Wax; Paraffin; Pressure

1. Introduction

Heavy paraffins precipitation in crude oils is mostly caused by cooling effects during production or during transport through pipelines traversing cold regions. So most of experimental works concerning wax formation were restricted to the measurement of the wax appearance temperatures or to the study of the temperature influence on wax content and composition in dead oil [1], fuel [2–4] or synthetic mixtures [5–7] under atmospheric pressure. In the same way, modelling studies have focused mainly on degassed oil [8–11], fuels [7,12] or synthetic systems [13,14] at atmospheric pressure.

* Corresponding author. Fax: +33-5-59-80-83-82.
E-mail address: jean-luc.daridon@univ-pau.fr (J.-L. Daridon).

0378-3812/00/$ - see front matter
PII: S0378-3812(99)00316-7

However, the presence of light gases in the live oil will greatly influence the phase behaviour of paraffinic crudes. In particular, the dissolution of light gases such as methane, ethane as well as carbon dioxide enhances the solubility of high molecular weight paraffins in liquid solvents [15]. Thus, gas pressurisation may decrease the wax appearance temperature by as much as 15 K from atmospheric pressure condition to the saturation pressure [16,17]. These changes, caused by gas dissolution and pressure effects, need to take into account both pressure and non-ideality of light–heavy solutions for modelling them.

The pressure effect on the behaviour of the fluid phases should be well described using a classical equation of state even in systems of compounds with large size differences. It is however well known that in spite of the good description of VLE, LLE or VLLE that can be achieved by a cubic EOS, these are unable to provide a correct description of the fugacities of the phases in equilibrium [18]. The good description is achieved because the fugacity deviations are identical in both fluid phases, thus cancelling the error. But when a solid phase is introduced in the system, and a model other than a cubic EOS is used for its description (an arbitrary G^E model for instance), the difference between the fugacity coefficients of the fluid and the solid phases becomes important, leading to a poor representation of the fluid–solid transitions [19,20]. To overcome this problem, an EOS–GE model was used in the description of the fluid phases. This approach removes the discrepancy in the fugacities between the fluid and solid phases.

Several equations of state coupled with an excess Gibbs energy model have been proposed for the prediction of vapor–liquid equilibria: Huron–Vidal [21], MHV2 [22], LCVM [23], Wong–Sandler [24]... However, it was found that the use of mixing rules from the LCVM model is able to describe accurately the liquid–vapor equilibrium for asymmetric systems [25], whereas both mixing rules Huron–Vidal and MHV2 leads, respectively, to an overvaluation and an underestimation of the bubble point.

In this study, a predictive procedure based on the LCVM model was developed for predicting solid–fluid and fluid–fluid phase equilibria at high pressures of synthetic systems containing light gases and a heavy fraction of paraffins ranging from C_{16} to C_{34}.

2. Procedure

Liquid–solid, liquid–vapor and liquid–vapor–solid phase equilibria under pressure may be described by the equality of the fugacity of individual components in all the different phases:

$$f_i^{\mathrm{V}}\left(T,P,x_i^{\mathrm{V}}\right) = f_i^{\mathrm{L}}\left(T,P,x_i^{\mathrm{L}}\right) = f_i^{\mathrm{S}}\left(T,P,x_i^{\mathrm{S}}\right) \qquad i = 1,2,\ldots,N \tag{1}$$

Using the liquid phase as the reference phase, the equilibrium ratios K_i^{V} and K_i^{S} can be defined as:

$$K_i^{\mathrm{V}} = \frac{\phi_i^{\mathrm{L}}(P)}{\phi_i^{\mathrm{V}}(P)} \tag{2}$$

$$K_i^{\mathrm{S}} = \frac{\phi_i^{\mathrm{L}}(P)}{\phi_i^{\mathrm{S}}(P)} \tag{3}$$

where coefficients ϕ_i^V, ϕ_i^L and ϕ_i^S correspond, respectively, to the fugacity coefficients in the vapor, liquid and solid phase.

2.1. Fluid phase modelling

The evaluation of liquid and vapor fugacity coefficients is carried out by an EOS/G^E model. Among the EOS/GE models available, the LCVM model [23] has been chosen because it yields a satisfactory prediction of high-pressure vapor–liquid equilibria of asymmetric light/heavy hydrocarbons systems [25]. The LCVM model is used with the SRK equation of state [26]:

$$P = \frac{RT}{(V-b)} - \frac{a}{V(V-b)}. \tag{4}$$

For mixtures, the conventional mixing rule is kept for the parameter b whereas the a parameter is related to the excess Gibbs energy according to the following relation:

$$\alpha = \left(\frac{a}{bRT}\right) = \left(\frac{\lambda}{A_v} + \frac{1-\lambda}{A_m}\right)\left(\frac{G^E}{RT}\right) + \frac{1-\lambda}{A_m}\sum_i x_i \ln\left(\frac{b}{b_i}\right)\sum_i x_i \alpha_i \tag{5}$$

where A_m, A_v and λ are constant. The excess Gibbs energy G^E of the liquid mixture is calculated using the Modified UNIFAC group contribution method with interaction parameters on the following form:

$$\Psi_{ij} = \exp\left(-\frac{A_{ij} + B_{ij}(T-298.15)}{T}\right). \tag{6}$$

The parameters used were fitted by Boukouvalas et al. [23,25] for the Original UNIFAC and are used here for the Modified UNIFAC. Although, rigorously, the interaction parameters should be refitted to the new combinatorial term, it was found, in agreement with other authors [27,28], that the same interaction parameters can be transferred between different UNIFAC versions where only the combinatorial term is changed.

The Modified UNIFAC has been preferred over the Original UNIFAC because it provides better results for asymmetric systems [29].

The critical properties required in the evaluation of the equation of state parameters come from the compilation of Reid et al. [30] for light gases whereas the Twu correlation [31] is used to predict the critical properties of the pure heavy components.

2.2. Solid phase modelling

The variation of the fugacity with pressure during a process at constant temperature can be evaluated by integration of the partial molar volume:

$$\ln f_i^S(P) = \ln f_i^S(P_0) + \frac{1}{RT}\int_{P_0}^{P} \overline{V_i^S}\, \mathrm{d}P \tag{7}$$

where $f_i^{S}(P_0)$ represents the solid fugacity at the reference pressure assumed to be the atmospheric pressure and $1/RT\int_{P_0}^{P}\overline{V_i^{S}}\,dP$ the Poynting term correction.

2.2.1. Solid fugacity at the reference pressure P_0

The solid fugacity at pressure P_0 from Eq. (7) can be evaluated in terms of activity coefficients:

$$f_i^{S}(P_0) = x_i^{S}\gamma_i^{S}(P_0)\,f_i^{S_0}(P_0) \tag{8}$$

where $f_i^{S_0}$ represents the fugacity of the pure solid at the same pressure and temperature.

The fugacity $f_i^{S_0}(P_0)$ of the component i in the pure solid reference state can be related to the pure subcooled liquid fugacity $f_i^{L_0}(P_0)$ from the change of energy between the pure solid and the liquid at temperature T [32]. Assuming the contribution of specific heat terms is negligible, the change of Gibbs energy can be expressed by:

$$\ln\frac{f_i^{S_0}(P_0)}{f_i^{L_0}(P_0)} = -\frac{\Delta G^{SL_0}}{RT} = -\frac{\Delta H^{SL_0}}{RT}\left(1-\frac{T}{T^{m}}\right) - \frac{\Delta H^{tr}}{RT}\left(1-\frac{T}{T^{tr}}\right) \tag{9}$$

where T^{m} and ΔH^{SL_0} represent, respectively the fusion temperature and the enthalpy of fusion whereas T^{tr} is the transition temperature and ΔH^{tr} the enthalpy of solid–solid transitions.

The activity coefficient of Eq. (8) that takes into account the deviation from the ideal behaviour is calculated using the Predictive Wilson equation [14,33], which provides a good description of the phase behaviour of waxy solutions [5]. For multi-component mixtures the activity coefficients are evaluated from:

$$\ln\gamma_i = 1 - \ln\sum_j x_j\Lambda_{ij} - \sum_k \frac{x_k\Lambda_{ki}}{\sum_j x_j\Lambda_{kj}} \tag{10}$$

with:

$$\Lambda_{ij} = \exp\left[-\frac{\lambda_{ij}-\lambda_{ji}}{RT}\right] \tag{11}$$

where the parameter λ_{ii} is estimated from the enthalpy of sublimation, ΔH^{SV}, by

$$\lambda_{ii} = -\frac{2}{Z}(\Delta H^{SV} - RT). \tag{12}$$

Assuming that the binary interaction depends only on the contact surface between two molecules, the parameter λ_{ij} is considered to be identical to the shorter molecule parameter λ_{ii} [14].

2.2.2. Poynting term correction

When the solid phase is composed by only one pure paraffin the partial molal volume is identical to the molar volume of the pure component:

$$\overline{V_i^{S}} = V_i^{S_0} \tag{13}$$

which can be taken proportional to the liquid molar volume [34] by the expression:

$$V_i^{S_0} = \beta V_i^{L_0} \tag{14}$$

Table 1
β value for multi-component solid phase

Average carbon number	V_s pure	V_l pure	β for mixture
16	22.281	25.908	0.909
17	23.554	27.388	0.906
18	24.826	28.867	0.904
19	26.0985	30.347	0.902
20	27.371	31.827	0.900
21	28.6435	33.306	0.898
22	29.916	34.786	0.897
23	31.1885	36.266	0.895
24	32.461	37.745	0.894
25	33.7335	39.225	0.892
26	35.006	40.705	0.891
27	36.2785	42.184	0.890
28	37.551	43.664	0.889
29	38.8235	45.144	0.888
30	40.096	46.623	0.887
31	41.3685	48.103	0.886
32	42.641	49.583	0.890
33	43.914	51.062	0.889
34	45.186	52.542	

with a proportionality coefficient β which is assumed pressure-independent and estimated to be equal to 0.86 for pure paraffins from the average value of the volume change data in the solid liquid phase transition by Shaerer et al. [34].

When the heavy fraction is made up by several *n*-alkanes, it is required to consider the excess volume of the mixture in order to adequately describe the $\overline{V_i^S}$ in the Poynting term. One way to include this excess volume in the calculation is to quantify its influence in the Poynting term through the value of β.

Considering the study made by Chevallier et al. [35], the difference in the crystal *c* parameter between the pure compounds and a mixed crystal of equivalent average carbon number, calculated from the Eq. (15), is approximately equal to one excess carbon atom for mixtures of paraffins ranging from C_{20} to C_{42}.

$$c_i = 0.2545\bar{n}_i + 0.3842 \tag{15}$$

This allows a reestimation of the β parameter to include the influence of the excess volume. As shown on Table 1 and Fig. 1, a value of $\beta = 0.90$ is a good choice for the multi-component heavy fraction. This explains why several authors [17,19,20,36] that dealt with this problem before found a value of $\beta = 0.90$ the optimal choice for this parameter without finding an explanation for the discrepancy between the value required for mixtures and for pure compounds.

The Poynting correction can thus be rewritten in terms of pure liquid fugacity at the pressure P as:

$$\text{Poynting term} = \frac{\beta}{RT}\int_{P_0}^{P} V_i^{L_0}\,dp = \beta \ln \frac{f_i^{L_0}(P)}{f_i^{L_0}(P_0)}. \tag{16}$$

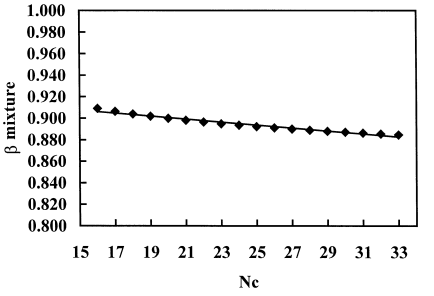

Fig. 1. Calculated β parameter for multi-component heavy fraction.

Finally, by combining Eqs. (7–9) and (16), the expression of the solid fugacity in the solid phase at the pressure P is given by:

$$f_i^{\mathrm{S}}(P) = \left(f_i^{\mathrm{L}_0}(P_0)\right)^{1-\beta}\left(f_i^{\mathrm{L}_0}(P)\right)^{\beta}\exp\left\{-\frac{\Delta H^{\mathrm{SL}_0}}{RT}\left(1-\frac{T}{T^{\mathrm{m}}}\right)-\frac{\Delta H^{\mathrm{tr}}}{RT}\left(1-\frac{T}{T^{\mathrm{tr}}}\right)\right\} \tag{17}$$

which can be rewritten in terms of equilibrium ratio:

$$K_i^{\mathrm{S}} = \frac{\phi_i^{\mathrm{L}}(P)\left(\phi_i^{\mathrm{L}_0}(P_0)\right)^{\beta-1}\left(\phi_i^{\mathrm{L}_0}(P)\right)^{-\beta}}{\gamma_i^{\mathrm{S}}(P_0)}\left(\frac{P}{P_0}\right)^{1-\beta} \times\exp\left\{\frac{\Delta H^{\mathrm{SL}_0}}{RT}\left(1-\frac{T}{T^{\mathrm{m}}}\right)+\frac{\Delta H^{\mathrm{tr}}}{RT}\left(1-\frac{T}{T^{\mathrm{tr}}}\right)\right\}. \tag{18}$$

2.2.3. Molar liquid volumes

The SRK equation of state is not satisfactory for liquid density calculations, and the Peneloux volume correction [37] is used to improve the prediction of liquid densities:

$$V = V' + C_i \tag{19}$$

where V' represents the volume calculated from the SRK equation of state and C_i is the translation parameter estimated at atmospheric pressure from a group contribution method [37]. The previous relation can be written in terms of fugacity coefficient:

$$\ln\phi_i^{\mathrm{L}}(P) = \ln\phi_i'^{\mathrm{L}}(P) + \left(\frac{C_i P}{RT}\right) \tag{20}$$

in which $\phi_i'^{\mathrm{L}}(P)$ represents the liquid fugacity coefficients calculated from the original SRK equation of state at pressure P.

Substitution of Eq. (20) into Eq. (18) will give the final liquid–solid equilibrium ratio of component i of the heavy fraction.

$$K_i^{\mathrm{S}} = \frac{\phi_i'^{\mathrm{L}}(P)\left(\phi_i'^{\mathrm{L}_0}(P_0)\right)^{\beta-1}\left(\phi_i'^{\mathrm{L}_0}(P)\right)^{-\beta}}{\gamma_i^{\mathrm{S}}}\left(\frac{P}{P_0}\right)^{1-\beta} \times\exp\left\{\frac{(1-\beta)C_i(P-P_0)}{RT}+\frac{\Delta H^{\mathrm{SL}_0}}{RT}\left(1-\frac{T}{T^{\mathrm{m}}}\right)+\frac{\Delta H^{\mathrm{tr}}}{RT}\left(1-\frac{T}{T_{\mathrm{tr}}}\right)\right\} \tag{21}$$

Table 2
Thermophysical properties used from correlation

Carbon number	T^{tr} (K)	T^{m} (K)	H^{tr} (J/mol)	H^{m} (J/mol)
16	277.3	289.2	9435.6	37,271.2
17	283.8	295.2	10,642.2	39,725.7
18	289.7	300.6	12,033.8	42,063.4
19	295.2	305.5	13,580.4	44,304.7
20	300.3	309.8	15,252.0	46,470.0
21	305.0	313.8	17,018.6	48,579.7
22	309.2	317.3	18,850.2	50,654.2
23	313.2	320.6	20,716.8	52,713.9
24	316.8	323.5	22,588.4	54,779.2
25	320.1	326.3	24,435.0	56,870.5
26	323.1	328.9	26,226.6	59,008.2
27	325.8	331.3	27,933.2	61,212.7
28	328.4	333.8	29,524.8	63,504.4
29	330.7	336.2	30,971.4	65,903.7
30	332.8	338.7	32,243.0	68,431.0
31	334.8	341.3	33,309.6	71,106.7
32	336.6	344.0	34,141.2	73,951.2
33	338.3	347.0	34,707.8	76,984.9
34	340.0	350.3	34,979.4	80,228.2

In this last expression the phase equilibrium ratio K_i^S is calculated only from liquid fugacity coefficients and from pure phase transition properties (T^m, T^{tr}, ΔH^{SL}, ΔH^{tr}, ΔH^{SV}, β) at low

Table 3
List of binary and ternary systems

Systems	Heavy component content range	Pressure range (MPa)	Number of points	References
C_1–C_{16}	0.1–0.9	3–80	50	Glaser et al. [44]
C_1–C_{20}	0.7–0.9	2–6	7	Puri and Kohn [45]
C_1–C_{20}	0.15–0.9	6–96	63	van der Kooi [46]
C_1–C_{22}	0.1–0.1	95–160	7	Flöter et al. [54]
C_1–C_{24}	0.1–0.75	10–205	87	Flöter et al. [47]
C_2–C_{16}	0.1–0.8	1–15	46	De Goede et al. [48]
C_2–C_{20}	0.1–0.8	0.6–3	11	Puri and Kohn [45]
C_2–C_{20}	0.1–0.9	0.5–11	78	Peters et al. [49]
C_2–C_{22}	0.1–0.8	1–10	47	Peters et al. [50]
C_2–C_{22}	0.1–0.65	1–4	6	Estrera and Luks [51]
C_2–C_{23}	0.1–0.75	0.5–4	10	Estrera and Luks [51]
C_2–C_{28}	0.1–0.9	0.5–5.5	11	Rodrigues and Kohn [52]
C_3–C_{34}	0.1–0.4	1–12	26	Peters et al. [53]
C_1–C_3–C_{24}	0.02–0.07	79–150	20	Flöter et al. [54]
C_1–C_{10}–C_{22}	0.053–0.199	0.1–45	38	Daridon et al. [55]
C_1–C_{10}–C_{32}	0.3–0.85	0.5–10	28	Cordeiro et al. [56]
C_2–C_{10}–C_{32}	0.83–0.85	0.1–0.6	6	Tan et al. [57]
C_1–C_{22}–C_{24}	0.03–0.1	95–175	106	Flöter et al. [54]

pressure. The liquid fugacity coefficients are calculated using the LCVM model whereas pure thermophysical properties come from literature data [38].

The correlation proposed by Lindeloff [39] is used for the evaluation of melting and transition temperatures and enthalpies. This correlation makes a distinction between the odd paraffins, crystallising in an orthorhombic lattice, and even paraffins in which the crystalline structure is triclinic or monoclinic. However, it is now evident [40–42] that in most cases the orthorhombic solid phase is the dominant solid crystalline structures for multi-component systems of *n*-paraffins, even if the mixed solid contains only even alkanes [39]. Thus, the odd paraffin correlation is extended by extrapolation to the ''orthorhombic even properties'' and, apart from pure even heavy fraction, only the odd correlation is used for predicting the pure properties of the paraffins of the mixed heavy fraction. Table 2 presents the thermophysical properties used in this work.

The phase boundaries are calculated using a procedure developed by Lindeloff [19,20] and are based in the multiphase flash algorithm developed by Michelsen [43].

3. Results and discussion

The proposed procedure allows both fluid–fluid and solid–fluid phase transitions calculation under pressure. However, only fluid–solid phase equilibria have been tested on binary and ternary systems

Table 4
Deviation ($T_{cal} - T_{exp}$) between experimental and calculated wax appearance temperatures for binary and ternary systems

Systems	Average deviation	Absolute average deviation
Methane – heavy paraffin binary systems		
C_1–C_{16}	1.18	1.2
C_1–C_{20}	0.27	1.13
C_1–C_{22}	−1.61	1.61
C_1–C_{24}	1.38	2.02
Ethane – heavy paraffin binary systems		
C_2–C_{16}	0.33	1.06
C_2–C_{28}	2.82	3.07
C_2–C_{20}	0.71	1.35
C_2–C_{22}	0.36	1.04
C_2–C_{23}	0.62	1.28
Propane – heavy paraffin binary systems		
C_3–C_{34}	2.07	2.07
Mixed solvent – heavy paraffin ternary systems		
C_1–C_3–C_{24}	1.07	1.83
C_1–C_{10}–C_{22}	0.11	0.34
C_1–C_{10}–C_{32}	1.12	2.09
C_2–C_{10}–C_{32}	−2.58	2.58
Methane – heavy paraffins ternary systems		
C_1–C_{22}–C_{24}	1.46	2.14
Global average absolute deviation		1.54

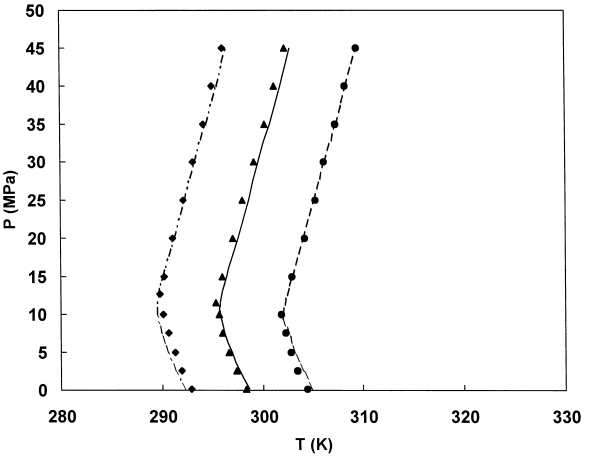

Fig. 2. Wax appearance temperatures calculated and measured for different compositions of the mixture C_1–C_{10}–C_{22}.

in this study, since liquid–vapor calculation remains identical to those from the LCVM model leading to a satisfactory description of vapor –liquid equilibria of light–heavy alkane systems [25].

3.1. Light gas–heavy paraffin binary systems

We concentrate first on light gas–heavy paraffin binary systems in which the heavy paraffin crystallises as a pure substance. These systems were used to test the ability of the EOS/G^E model approach to predict the high pressure fluid–solid equilibria in a situation where the deviations from experimental data cannot be attributed to the errors in the description of the solid phase non-ideality as $\gamma_i^S = 1$. Specifically, the binary systems tested, which are listed in Table 3, include either methane, ethane or propane with paraffins ranging between C_{16} and C_{34} for which the fluid–solid phase

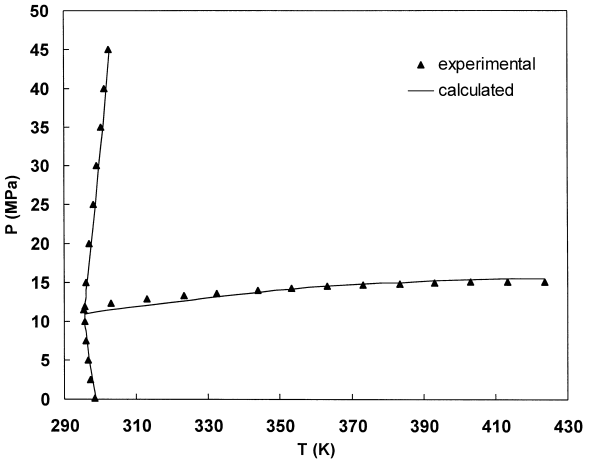

Fig. 3. Phase envelope of the C_1–C_{10}–C_{22}.

Table 5
Feed composition (mass %) of the $C_1 + C_{10}$ + distribution of paraffin systems

	Mix a	Mix b	Mix c	Mix d
Full composition				
% of methane	43.7	43.8	43.6	44.0
% of decane	46.1	45.9	46.15	45.8
% of heavy fraction	10.2	10.3	10.25	10.2
Composition of heavy fraction				
% of *n*-C_{18}	–	16.04	12.93	66.67
% of *n*-C_{19}	–	13.90	12.38	–
% of *n*-C_{20}	32.02	12.18	11.30	–
% of *n*-C_{21}	21.92	11.14	10.78	–
% of *n*-C_{22}	15.04	8.81	10.13	–
% of *n*-C_{23}	10.28	7.57	9.55	–
% of *n*-C_{24}	7.04	6.53	9.00	–
% of *n*-C_{25}	4.82	5.60	8.47	–
% of *n*-C_{26}	3.31	4.85	7.95	–
% of *n*-C_{27}	2.25	4.14	7.51	–
% of *n*-C_{28}	1.54	3.56	–	–
% of *n*-C_{29}	1.06	3.05	–	–
% of *n*-C_{30}	0.72	2.63	–	33.33

behaviour was available [44–54] at pressures up to 200 MPa. The deviations from experimental data are displayed in Table 4, which provides the average deviation (AD) and absolute average deviation (AAD) for each binary system as well as for the full set of data tested. It can be shown that the proposed approach, which rest on an equation of state/G^E model developed primarily to calculate liquid–vapor equilibria, gives a satisfactory representation of fluid–solid equilibria with an average absolute deviation of 1.5 K. The method provides a good estimation of the slope of the melting line at pressure above the bubble pressure, indicating that the pressure effects are well described by the model.

3.2. Mixed solvent–heavy paraffin ternary systems

Further comparisons have been performed on ternary systems made up of a mixed solvent and a single heavy paraffin (Table 3). The first ternary system [54] included in the test is formed by a

Table 6
Deviation ($T_{cal} - T_{exp}$) between experimental and calculated wax appearance temperatures for multi-component systems

Systems	Average deviation	Absolute average deviation
Distribution A	0.18	0.20
Distribution B	−0.10	0.14
Distribution C	−1.05	1.05
Distribution D	−0.53	0.53

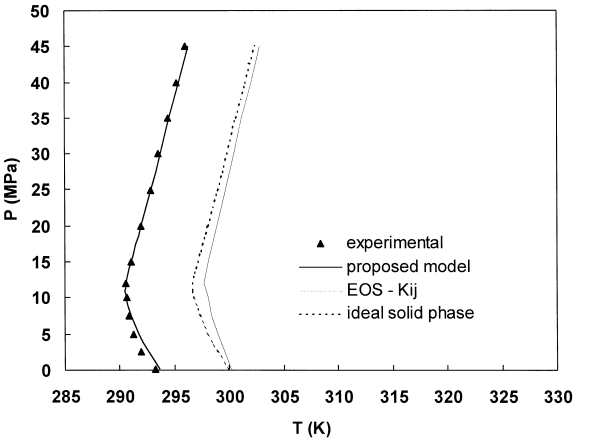

Fig. 4. Wax appearance temperatures measured and calculated from three different approaches of multi-component mixture A.

mixture of two gases (methane + propane) plus various proportions of tetracosane, whereas the others [54–57] are made up of a gas (methane or ethane) with an intermediate solvent (decane) and a heavy component. The results are presented in Table 4. They show that for these systems the results obtained are similar to those obtained with binary mixtures, meaning that the nature and the number of solvents does not influence the quality of the phase behaviour description. Again the pressure dependence is well described by the model as it can be observed on Fig. 2 where only the fluid–solid transition lines are represented for three different compositions of the system C_1–C_{10}–C_{22}.

The phase envelope of one of the mixture of C_1–C_{10}–C_{22} is plotted in Fig. 3, including the liquid–vapor transitions as well as the fluid– solid transition.

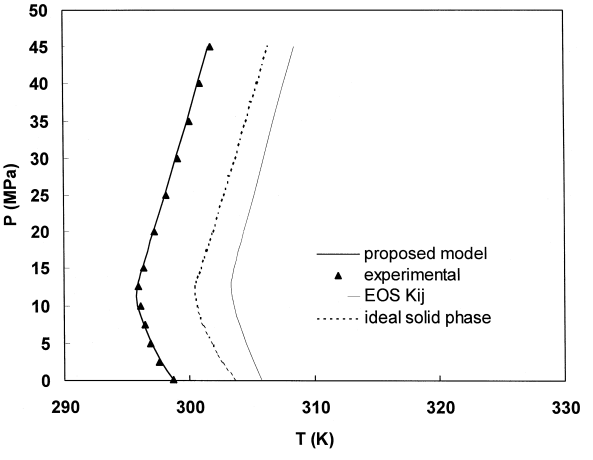

Fig. 5. Wax appearance temperatures measured and calculated from three different approaches of multi-component mixture B.

Table 7
AD% and AAD% between experimental and calculated bubble points for multi-component systems

Systems	Average deviation %	Absolute average deviation %
Distribution A	−0.73	3.25
Distribution B	−3	4.00
Distribution C	−1.3	2.99
Distribution D	−2.39	2.70

3.3. Light gas–intermediate solvent–multi-paraffin systems

A set of systems, where the heavy fraction is formed from several heavy components, has been tested in order to study the capacity of the model for systems where the heavy fraction is not restricted to one component. The fluid–solid equilibrium data come from phase boundary measurements carried out up to 50 MPa on synthetic mixtures whose composition is close to those encountered in natural fluids [58]. These complex systems (Table 5) are mainly made up of a mixed solvent methane + decane (with a molar fraction of methane of about 50%) and 10% of a distribution of heavy normal paraffins centred around C_{22} with a molar concentration regularly decreasing from C_{18} to C_{30}.

The model deviations in the prediction of the solid–fluid phase boundary for each of these systems are presented in the Table 6. The results are remarkably good both below and above the bubble point pressure. Maximum deviations appear at the triple point and are in all cases inferior to 1.5 K. A comparison with the results obtained using the proposed model with two other modelling approaches are presented in Figs. 4 and 5.

Firstly, a comparison has been made with a calculation based on a cubic equation of state with classical quadratic mixing rules, coupled with the Wilson equation for the description of the solid phase [19,20]. The deviations are as larger as 10 K, indicating that the fluid phase description used is required to obtain a real continuity of the fugacity coefficients in the different phases in equilibrium.

The second comparison was done by assuming that the solid phase is ideal. The results show the importance of an adequate description of solid phase non-ideality for paraffinic solutions.

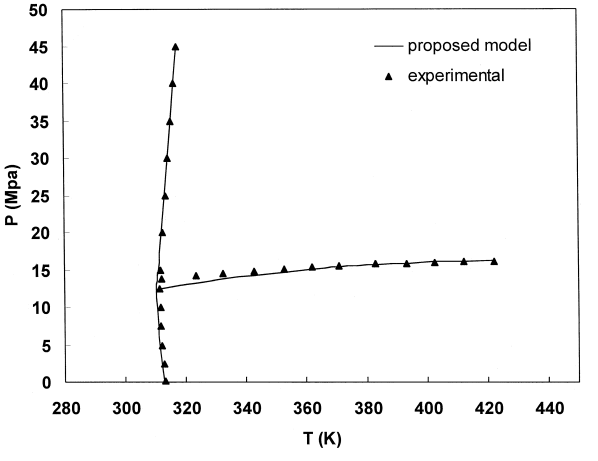

Fig. 6. Measured and calculated phase envelope of the C_1–C_{10}–multi-paraffin system C.

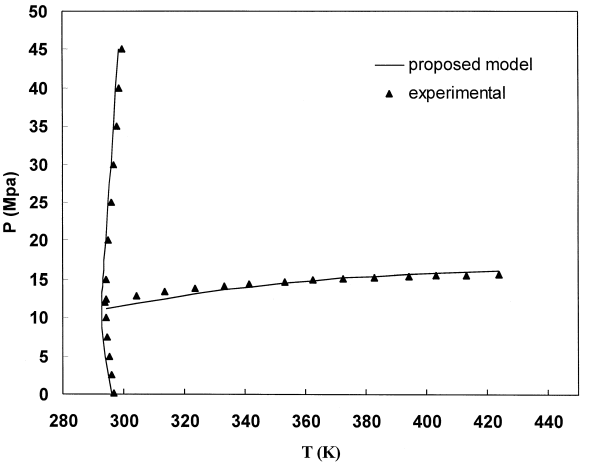

Fig. 7. Measured and calculated phase envelope of the C_1–C_{10}–multi-paraffins system D.

The model deviations in the prediction of the fluid–fluid phase boundary for each of these systems are presented in the Table 7. In Figs. 6 and 7 the phase envelope, including the bubble point line, is presented for mixtures C and D. Both fluid–fluid and solid–fluid phase boundaries are well described.

4. Conclusion

The results presented show that the proposed approach provides an excellent description of both fluid–fluid and solid–fluid phase boundaries of paraffinic solutions. This is achieved by removing two problems of previous approaches: (1) Using an adequate description of the solid phase non-ideality; (2) guaranteeing the continuity of the fugacities between the solid and fluid phases using an EOS/GE model instead of a cubic EOS with quadratic mixing rules. A rigorous introduction of the excess volumes in the Poynting correction was also done. This provides an adequate representation of the effect of the pressure on the solid phase non-ideality.

List of symbols

a, b	equation of state parameters
A	mixing rule parameter
f	fugacity
G	Gibbs free energy
H	enthalpy
K	equilibrium ratio
P	pressure
R	ideal gas constant
T	temperature
V	volume
x_i	mole fraction of i

Greek letters

β	volume change parameter
ϕ	fugacity coefficient
γ	activity coefficient
λ	interaction parameters of Wilson equation
Ψ	interaction parameters of UNIFAC

Superscripts

E	Excess
L	liquid
m	melting
tr	transition
r	reference phase
S	solid
SL	solid–liquid phase change
SV	solid–vapor phase change
V	vapor
′	Properties calculated from the SRK equation of state
–	Partial properties

Subscripts

i	component
n	carbon number
0	pure component

Acknowledgements

The authors want to thank to Dr. G.M. Kontogeorgis for helpful discussions on EOS, and in particular LCVM.

References

[1] W.B. Pedersen, A.B. Hansen, E. Larsen, A.B. Nielsen, Energy Fuels 5 (1991) 908.
[2] C.T. Moynihan, R. Mossadegh, A.J. Bruce, Fuel 63 (1984) 378.
[3] T.L. van Winkle, W.A. Affens, E.J. Beal, G.W. Mushrush, R.N. Hazlett, J. DeGuzman, Fuel 66 (1987) 890.
[4] J.A.P. Coutinho, C. Dauphin, J.L. Daridon, Fuel (1999) in press.
[5] J. Pauly, C. Dauphin, J.L. Daridon, Fluid Phase Equilib. 149 (1998) 191.
[6] C. Dauphin, J.L. Daridon, J.A.P. Coutinho, P. Baylère, M. Potin-Gautier, Fluid Phase Equilib. 161 (1999) 135–151.
[7] J.A.P. Coutinho, V. Ruffier-Meray, Ind. Eng. Chem. Res. 36 (1997) 4977–4983.
[8] K.W. Won, Fluid Phase Equilib. 30 (1986) 265.
[9] J.H. Hansen, Aa. Fredenslund, K.S. Pedersen, H.P. Ronningsen, AIChE J. 34 (1988) 1937.
[10] K.S. Pedersen, P. Skovborg, H.P. Ronningsen, Energy Fuels 5 (1991) 924.
[11] C. Lira-Galena, A. Firoozabadi, J.M. Prausnitz, AIChE J. 42 (1996) 239.
[12] J.A.P. Coutinho, Energy Fuels, submitted for publication.
[13] J.A.P. Coutinho, S.I. Andersen, E.H. Stenby, Fluid Phase Equilib. 103 (1995) 23.

[14] J.A.P. Coutinho, K. Knudsen, S.I. Andersen, E.H. Stenby, Chem. Eng. Sci. 51 (1996) 3273.
[15] V. Ruffier Meray, J.L. Volle, C.J.P. Schranz, P. Le Marechal, E. Behar, SPE J. (1993) 26549.
[16] H. Pan, A. Firoozabadi, P. Fotland, SPE Prod. Facil. (1993) 250, Nov.
[17] H.P. Roenningsen, B.F. Soemme, K.S. Pedersen, Proceedings from Multiphase '97, BHR Group, 1997.
[18] L. Lundgaard, J. Mollerup, Fluid Phase Equilib. 70 (1991) 199.
[19] N. Lindeloff, E.H. Stenby, K. Knudesen, J.L. Daridon, CHISA'96 Meeting, Praha, Czech Republic, August 25–30, 1996.
[20] N. Lindeloff, R.A. Heidemann, S.I. Andersen, E.H. Stenby, Ind. Eng. Chem. Res. 38 (1999) 1107–1113.
[21] M.J. Huron, J. Vidal, Fluid Phase Equilib. 3 (1979) 255.
[22] S. Dahl, Aa. Fredenslund, P. Rasmussen, Ind. Eng. Chem. Res. 30 (1991) 1936.
[23] C.J. Boukouvalas, N. Spiliotis, Ph. Coustikos, N. Tzouvaras, D.P. Tassios, Fluid Phase Equilib. 92 (1994) 75.
[24] D.S.H. Wong, S.I. Sandler, AIChE J. 38 (1992) 671–680.
[25] C.J. Boukouvalas, K.G. Magoulas, S.K. Stamataki, D. Tassios, Ind. Eng. Chem. Res. 36 (1997) 5454.
[26] G. Soave, Chem. Eng. Sci. 27 (1972) 1197–1203.
[27] G.M. Kontogeorgis, Aa. Fredenslund, D. Tassios, Ind. Eng. Chem. Res. 32 (1993) 362–372.
[28] J.A.P. Coutinho, E.H. Stenby, Ind. Eng. Chem. Res. 35 (1996) 918.
[29] I. Kikic, P. Alessi, P. Rasmussen, Aa. Fredenslund, Can. J. Chem. Eng. 8 (1980) 253–258.
[30] R.C. Reid, J.M. Prausnitz, B.E. Poling, The Properties of Gases and Liquids, 4th edn.,1987.
[31] C.H. Twu, Fluid Phase Equilib. 16 (1984) 137.
[32] J.M. Prausnitz, Molecular Thermodynamics of Fluid Phase Equilibria, Prentice-Hall, Englewood Cliffs, New Jersey, 1969.
[33] G.M. Wilson, J. Am. Chem. Soc. 86 (1964) 127.
[34] A.A. Schaerer, C.J. Busso, A.E. Smith, L.B. Skinner, J. Am. Chem. Soc. 77 (1986) 2017.
[35] V. Chevallier, E. Provost, J.B. Bourdet, M. Boukoukba, D. Petitjean, M. Dirand, Polymer 40 (1999) 2121–2128.
[36] P. Ungerer, Fluid Phase Equilib. 111 (1995) 287.
[37] A. Peneloux, E. Rauzy, R. Frèze, Fluid Phase Equilib. 8 (1982) 7.
[38] M.G. Broadhurst, J. Res. Nat. Bur. Stand. 66A (1962) 241–249.
[39] N. Lindeloff, MsC Thesis, Denmark, 1996.
[40] S.R. Craig, G.P. Hastie, K.J. Roberts, A.R. Gerson, J.N. Sherwood, R.D. Tack, J. Mater. Chem. 8 (1998) 859.
[41] M. Dirand, V. Chevallier, E. Provost, M. Bouroukba, D. Petitjean, Fuel 77 (1998) 1253–1260.
[42] V. Chevallier, D. Petitjean, M. Bouroukba, M. Dirand, Polymer 40 (1999) 2129–2137.
[43] M.L. Michelsen, Comput. Chem. Eng. 18 (1994) 7.
[44] M. Glaser, C.J. Peters, H.J. van der Kooi, J. Chem. Thermodyn. 17 (1985) 803.
[45] S. Puri, J.P. Kohn, J. Chem. Eng. Data 15 (1970) 372.
[46] H.J. van der Kooi, E. Flöter, J. Chem. Thermodyn. 27 (1995) 847–861.
[47] E. Flöter, Th.W. de Loos, J. de Swaan, Fluid Phase Equilib. 127 (1997) 129.
[48] R. De Goede, C.J. Peters, H.J. van der Kooi, R.N. Lichtenthaler, Fluid Phase Equilib. 50 (1989) 305.
[49] C.J. Peters, J.L. de Roo, R.N. Lichtenthaler, Fluid Phase Equilib. 65 (1991) 135.
[50] C.J. Peters, J. Spiegelaar, J. de Swaan Arons, Fluid Phase Equilib. 41 (1988) 245–256.
[51] S.S. Estrera, K.D. Luks, Am. Chem. Soc. 21 (1987) 201.
[52] A.B. Rodrigues, J.P. Kohn, 12(1967), 191.
[53] C.J. Peters, J.L. de Roo, J. de Swaan Arons, Fluid Phase Equilib. 72 (1992) 251–266.
[54] E. Flöter, B. Hollanders, T.W. de Loos, J. de Swaan Arons, Fluid Phase Equilib. 143 (1998) 185.
[55] J.L. Daridon, D. Bessieres, P. Xans, High Temp.–High Pressures 29 (1997) 337–344.
[56] D.J. Cordeiro, K.D. Luks, J.P. Kohn, Ind. Eng. Chem. Process Des. Dev. 12 (1973) 47.
[57] F.O. Tan, D.J. Cordeiro, K.D. Luks, J.P. Kohn, AIChE J. 19 (1973) 847.
[58] J.L. Daridon, P. Xans, F. Montel, Fluid Phase Equilib. 117 (1996) 241.